

NOTE

## Crystal Structures of Thermally Stable Adenylate Kinase Mutants Designed by Local Structural Entropy Optimization and Structure-guided Mutagenesis

Sojin Moon · Euiyoung Bae

Received: 25 July 2014 / Accepted: 14 August 2014 / Published Online: 31 October 2014  
© The Korean Society for Applied Biological Chemistry and Springer 2014

**Abstract** Thermally stable proteins are desirable in many industrial and laboratory settings, and numerous approaches have been developed to redesign proteins for higher thermal stability. Here, we report the crystal structures of two thermally stable adenylate kinase (AK) mutants that were designed by applying a combination of local structural entropy (LSE) optimization and structure-guided mutagenesis. Structure-guided mutagenesis resulted in stabilizing interactions connecting distant regions of the LSE-optimized AK sequence. This demonstrates the feasibility and importance of simultaneous optimization of local and global features in protein thermal stabilization. An additional AK mutant showed that small changes in side-chain configuration can greatly impact thermal stability.

**Keywords** adenylate kinase · local structural entropy · mutagenesis · protein stability · structural biology

### Introduction

Thermally stable proteins maintain structural integrity and can perform biological functions at elevated temperatures. Such traits are desirable in many industrial and laboratory settings (Daniel and Danson, 2010). Numerous approaches have been developed to increase the thermal stability of various target proteins (Liszka et al., 2012). One such approach is structure-based rational design involving site-directed mutagenesis (Eijsink et al., 2004). In this method, mutations are introduced to optimize stabilizing structural

features such as ion pairs, hydrogen bonds, and hydrophobic packing. Despite many successes, this method requires detailed structural information of target proteins to identify the necessary mutations, which makes the method difficult to generalize and automate.

We previously developed a stabilization method based on measures of local structural entropy (LSE) (Bae et al., 2008). LSE is an empirical descriptor of conformational variability in a protein sequence (Chan et al., 2004) that is computed based on structural information derived from the Protein Data Bank (PDB) (Berman et al., 2000). Reducing the LSE of a protein sequence by introducing mutations can result in fewer conformational states and thus a more stable structure (Bae et al., 2008). This approach does not require structural information of the target proteins but is limited by the fact that LSE overlooks and can damage global stabilizing structural features connecting distant regions of a polypeptide (Moon et al., 2014a).

In our previous study, we generated adenylate kinase (AK) mutants with enhanced thermal stability by combining LSE optimization and structure-guided mutagenesis (Fig. 1A) (Moon et al., 2014a). We designed an LSE-optimized AK variant (AKlse, formerly known as AKlse4) by substituting residues from a mesophilic *Bacillus subtilis* AK (AKmeso) with those of psychrophilic *Bacillus globisporus* and thermophilic *Geobacillus stearothermophilus* AKs (AKpsycrho and AKthermo, respectively). Using this AKlse as a template, two additional stable AK mutants (AKm1 and AKm2, formerly known as AKlse4m1 and AKlse4m2, respectively) were generated, on which structure-guided mutagenesis was performed to introduce global stabilizing elements, such as ion pairs and hydrophobic interactions.

This study describes the crystal structures of AKm1 and AKm2, in which mutated residues form stabilizing interactions that connect distant regions of the polypeptide on the LSE-optimized template. We also designed another AK mutant, AKm3, and found that a small change in side-chain configuration can have a significant effect on thermal stability. Taken together, these results show that local

S. Moon  
Department of Agricultural Biotechnology, Seoul National University,  
Seoul 151-921, Republic of Korea

E. Bae (✉)  
Department of Agricultural Biotechnology, Center for Food and  
Bioconvergence, and Research Institute of Agriculture and Life Sciences,  
Seoul National University, Seoul 151-921, Republic of Korea  
E-mail: bae@snu.ac.kr

and global stabilizing features can be optimized simultaneously, a finding that may serve as a general principle for protein thermal stabilization studies.

## Materials and Methods

### Purification and thermal denaturation midpoint ( $T_m$ ) measurement.

AK mutant constructs were generated by polymerase chain reactions using mismatched primers. The synthetic AKlse gene in a pET11a vector was used as a template. The mutant proteins were overexpressed in *Escherichia coli* and purified by a two-step procedure involving affinity chromatography and size exclusion chromatography, as described previously (Moon et al., 2014b). To determine  $T_m$ , circular dichroism spectroscopy was used, as described previously (Moon et al., 2014b).

**Crystallization.** Crystals were grown at 20°C by the hanging-drop method with 4 mM P<sup>1</sup>,P<sup>5</sup>-di(adenosine 5')-pentaphosphate (Ap<sub>5</sub>A) in buffer (10 mM HEPES pH 7.0). AKm1 (30 mg/mL) was mixed with an equal amount of a reservoir solution containing 18% (w/v) polyethylene glycol 3350, 100 mM lithium sulfate, and 100 mM Bis-Tris pH 5.5. Crystals of AKm2 (18 mg/mL) were obtained from a reservoir solution including 22% (w/v) polyethylene glycol 3350 and 200 mM calcium chloride. The crystals were cryoprotected in the reservoir solutions supplemented with 20% (v/v) glycerol and flash-frozen in liquid nitrogen.

**Data collection, phasing and refinement.** Diffraction data for AKm1 and AKm2 were collected at 100 K at beamlines 7A and 5C, respectively, of the Pohang Accelerator Laboratory. The diffraction images were processed using HKL2000 (Otwinowski and Minor, 1997). Previously solved AK structures (PDB codes 4MKG and 1ZIO, respectively) were used as starting models for molecular replacement phasing in Phaser (McCoy et al., 2007) for AKm1 and Molrep (Vagin and Teplyakov, 2010) for AKm2. The structures were completed using alternate cycles of manual fitting in COOT (Emsley and Cowtan, 2004) and refinement in REFMAC5 (Murshudov et al., 1997). The stereochemical quality of the final models was assessed using MolProbity (Chen et al., 2010).

**Accession numbers.** The atomic coordinates and structure factors of AKm1 and AKm2 were deposited in the PDB (Berman et al., 2000) with the accession codes 4TYP and 4TYQ, respectively.

## Results and Discussion

**Structure determination of AK mutants.** The LSE-optimized AK variant, AKlse, and the two AKlse-based mutants, AKm1 and AKm2, were designed and their  $T_m$  values were measured in a previous study (Table 1) (Moon et al., 2014a). AKlse was generated by reducing the LSE of AKmeso in the CORE domain, which controls almost exclusively the overall stability of AK (Bae and Phillips, 2006). To produce AKm1, three ion pairs (Lys19-Glu202, Arg116-Glu198, and Lys180-Asp114) were introduced into AKlse. In AKm2, the His109, Arg193, and Leu211 residues of AKlse were substituted with Tyr, Val, and Ile residues, respectively, to optimize hydrophobic contacts.

To verify the structural basis of the increased thermal stabilities of AKm1 and AKm2 relative to that of AKlse, whose structure (PDB code 4QBG) was solved previously (Moon et al., 2014b), we determined the crystal structures of AKm1 and AKm2 to resolutions of 2.90 and 1.65 Å, respectively (Fig. 1B). Data collection and refinement statistics are summarized in Table 2. The asymmetric unit of AKm1 includes four polypeptide chains while two chains were identified in the structure of AKm2.

The chain folds of AKm1 and AKm2 are essentially identical to those of other AKs, including AKlse (Fig. 1B). They display the characteristic AK domain arrangement with the bound inhibitor Ap<sub>5</sub>A in the active site. The root-mean-square-deviation (RMSD) values of C $\alpha$  atoms between AKlse and each of the two mutants, AKm1 and AKm2, ranged from 1.2 to 2.0 Å. Thus, it is most likely that the differences in thermal stability between the AKlse mutants and their template, AKlse, result from relatively small structural changes caused by the mutations introduced to form stabilizing interactions connecting distant regions of the polypeptide.

**Introduction of ion pairs connecting distant regions of AKm1.** In the process of generating AKm1 using AKlse as a template, mutations were introduced in order to construct three ion pairs (Lys19-Glu202, Arg116-Glu198, and Lys180-Asp114) (Moon et al., 2014a). These ion pairs were originally found in the structure of AKthermo and connect distant regions (>10 residues) in the AKthermo sequence (Bae and Phillips, 2004). In AKlse, the ion pairs are not tightly maintained or lost by residue mutations to uncharged amino acids (Moon et al., 2014a).

**Table 1** Summary of the AK mutants used in this study

	Design strategy	$T_m$ (°C)	$\Delta T_m$ (°C) <sup>a</sup>
AKlse	LSE optimization	56.6 <sup>b</sup>	N/A
AKm1	Ion pairs (Lys19-Glu202, Arg116-Glu198, and Lys180-Asp114) added on AKlse	58.4 <sup>b</sup>	1.8
AKm2	Hydrophobic residues (Tyr109, Val193, and Ile211) added on AKlse	58.2 <sup>b</sup>	1.6
AKm3	Hydrophobic residues (Tyr109 and Val193) added on AKlse	56.7	0.1

<sup>a</sup>Difference from  $T_m$  of AKlse.

<sup>b</sup>From Moon et al., 2014a.

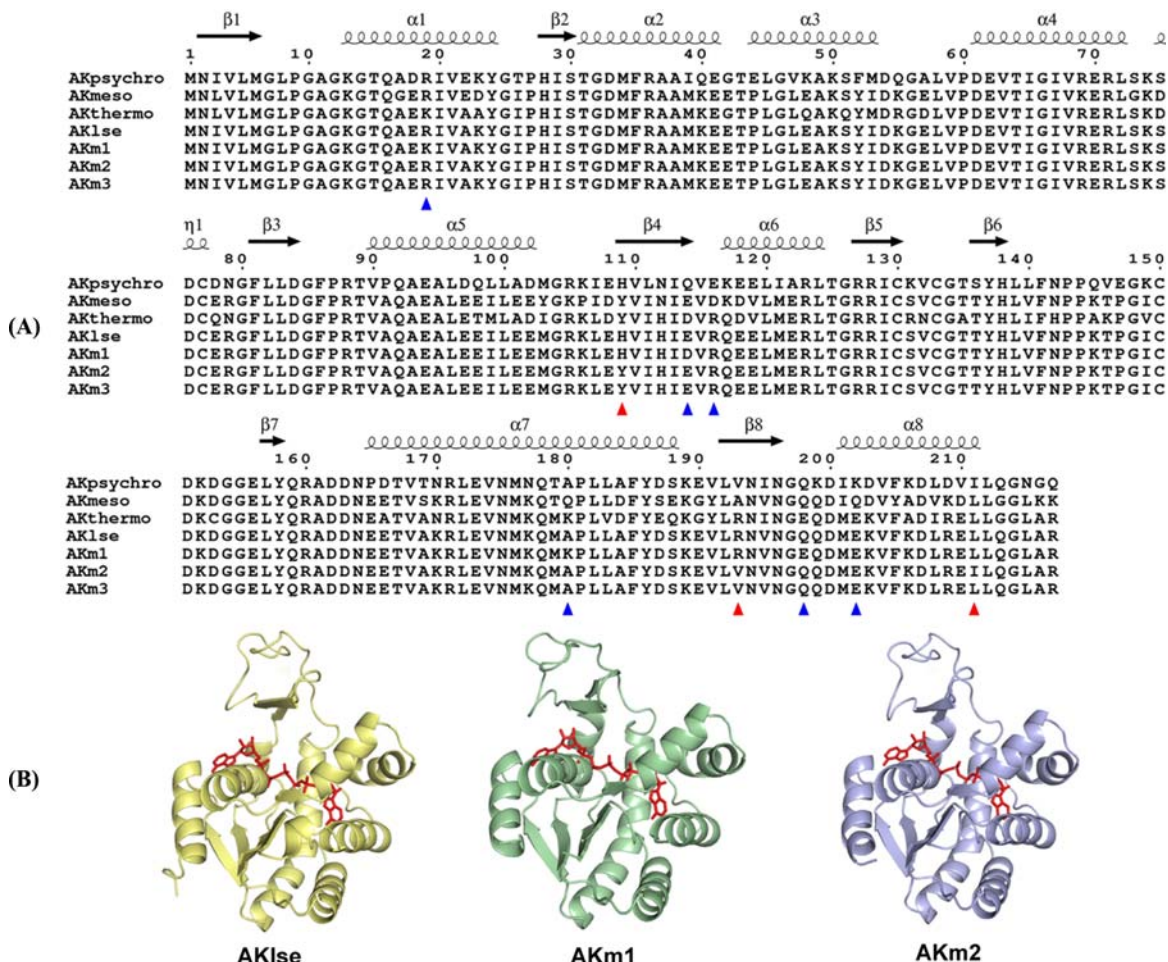


**Fig. 1** Sequence alignment and structures of thermally stable AK mutants. (A) Sequence alignment of three wild-type AKs, AKlse, and three AKlse mutants. Mutated residues for ion pairs and hydrophobic contacts are indicated by blue and red triangles, respectively. Secondary structures are indicated based on the structure of AKlse. (B) Overall structures of AKlse (yellow), AKm1 (green), and AKm2 (purple). Bound Ap<sub>5</sub>A inhibitor molecules are also shown in red.

In the structure of AKm1, oppositely charged side chains of the Lys19-Glu202 and Arg116-Glu198 ion pairs were found within close proximity to each other (Figs. 2A and B), indicating that these two ion pairs are tightly maintained and serve to connect distant regions of the AKm1 polypeptide. The average distances between the positively and negatively charged atoms in the Lys19-Glu202 and Arg116-Glu198 ion pairs are 4.21 and 3.17 Å, respectively, for the four independent chains in the crystal structure of AKm1.

Conversely, the Lys180-Asp114 ion pair does not seem to be formed in AKm1 since the distance between the two oppositely charged atoms is greater than 9 Å in all four of the AKm1 chains. This is consistent with the results of our previous AKthermo study (Bae and Phillips, 2005). In a molecular dynamics simulation of AKthermo, the Lys180-Asp114 ion pair was not maintained within a short distance, suggesting that the formation of the Lys180-Asp114 ion pair in AKthermo might be a crystallographic artifact caused by the packing of neighboring molecules in the crystal lattice (Bae and Phillips, 2005).

Thus, the structure of AKm1 showed that two (Lys19-Glu202 and Arg116-Glu198) of the three ion pairs were successfully introduced into an LSE-optimized template by structure-guided mutagenesis, suggesting that these two ion pairs likely contribute to the increased thermal stability of AKm1 compared to that of its template, AKlse. In our previous study, the introduction of the Lys19-Glu202 and Arg116-Glu198 ion pairs increased the *T<sub>m</sub>* value of AKmeso. In contrast, the Lys180-Asp114 ion pair did not have any effect on thermal stability when incorporated into AKmeso (Bae and Phillips, 2005).

**Optimization of hydrophobic contacts for thermal stabilization in AKm2.** In AKm2, the His109, Arg193, and Leu211 of AKlse were replaced with more hydrophobic amino acids (Tyr109, Val193, and Ile211) to optimize the hydrophobic interactions between distant polypeptide regions (Moon et al., 2014a). Tyr, Val, and Ile were selected for mutation based on sequence alignments with wild-type AKs (Fig. 1A). In the crystal structure of AKm2 (Fig. 2C), the hydrophobic side chain atoms of the three mutated residues

**Table 2** Data collection and refinement statistics<sup>a</sup>

	AKm1	AKm2
Space group	P2 <sub>1</sub>	P1
Unit cell parameters (Å)	a=43.6, b=123.3, c=86.7, β=98.3°	a=39.0, b=48.8, c=54.8, α=90.0°, β=97.3°, γ=95.8°
Wavelength (Å)	0.97934	0.97960
<b>Data collection statistics</b>		
Resolution range (Å)	50.00–2.90 (3.00–2.90)	50.00–1.65 (1.71–1.65)
Number of reflections	18989 (1878)	45746 (4395)
Completeness (%)	94.0 (94.1)	95.7 (92.3)
R <sub>merge</sub> <sup>b</sup>	0.164 (0.611)	0.074 (0.198)
Redundancy	3.5 (3.6)	1.9 (1.9)
Mean I/σ	5.9 (2.3)	8.4 (4.6)
<b>Refinement statistics</b>		
Resolution range (Å)	50.00–2.90	50.00–1.65
R <sub>cryst</sub> <sup>c</sup> /R <sub>free</sub> <sup>d</sup> (%)	29.0/32.9	17.8/21.9
RMSD bonds (Å)	0.010	0.021
RMSD angles (°)	1.303	2.246
Average B factor (Å <sup>2</sup> )	42.46	18.73
Number of water molecules	13	332
Ramachandran favored (%)	96.9	99.8
Ramachandran allowed (%)	3.1	0.2

<sup>a</sup>Values in parentheses are for the highest-resolution shell.

<sup>b</sup>R<sub>merge</sub> =  $\sum_h \frac{1}{\Sigma_i |I_i(h)|} - \langle |I(h)| \rangle / \Sigma_h \Sigma_i |I_i(h)|$ , where I<sub>i</sub>(h) is the intensity of an individual measurement of the reflection and  $\langle |I(h)| \rangle$  is the mean intensity of the reflection.

<sup>c</sup>R<sub>cryst</sub> =  $\sum_h \frac{|F_{obs}| - |F_{calc}|}{|F_{obs}|} / \Sigma_h |F_{obs}|$ , where F<sub>obs</sub> and F<sub>calc</sub> are the observed and calculated structure factor amplitudes, respectively.

<sup>d</sup>R<sub>free</sub> was calculated as R<sub>cryst</sub> using 5% of the randomly selected unique reflections that were omitted from structure refinement.

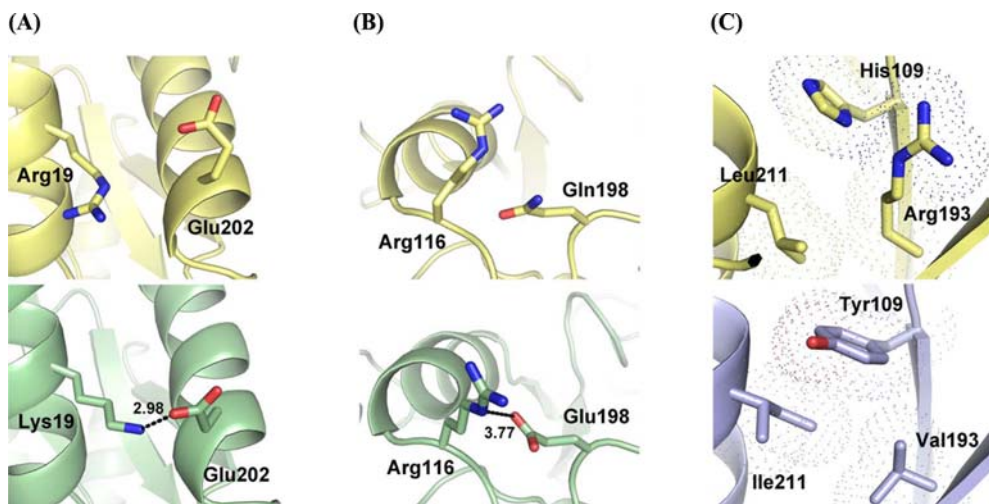


**Fig. 2** Optimization of stabilizing interactions connecting distant polypeptide regions. Lys19–Glu202 (A) and Arg116–Glu198 (B) ion pairs were formed in AKm1 (green). (C) Hydrophobic packing was improved by incorporating Tyr109, Val193, and Ile211 into AKm2 (purple). For side-chain atoms, van der Waals surfaces are represented. Equivalent residues in AKlse (yellow) are shown for comparison.

make close hydrophobic contacts over relatively short distances (<4.5 Å). This suggests that the enhanced thermal stability of AKm2, compared to AKlse, results from the improved hydrophobic packing of residues from distant regions of the polypeptide.

We also designed another AKlse mutant, AKm3, and tested its thermal stability by measuring its  $T_m$  value (Table 1 and

Supplementary Fig. 1). In AKm3, the His109 and Arg193 of AKlse were replaced with Tyr and Val residues, respectively, as in AKm2, but Leu211 was not changed. Despite the two mutated residues, the  $T_m$  value of AKm3 (56.7°C) was only 0.1°C higher than that of its template, AKlse (Table 1). This result indicates that these mutations did not increase the thermal stability of AKm3

and suggests that an Ile-to-Leu substitution can disrupt optimal hydrophobic packing. In more general terms, our results imply that small changes in side-chain configuration can have a considerable effect on the overall thermal stability of a protein.

This study demonstrated that mutations designed to construct non-covalent interactions connecting distant polypeptide regions can effectively increase the thermal stability of an LSE-optimized protein target. Our results highlight the feasibility and importance of the simultaneous optimization of local and global features in protein thermal stabilization.

**Acknowledgments** We thank the structural biology beamline staff of the Pohang Accelerator Laboratory for their support with data collection. This work was supported by the Basic Science Research Program through the National Research Foundation of Korea (NRF) funded by the Ministry of Education, Science and Technology (2009-0067791) and the Seoul National University Research Grant.

## References

- Bae E and Phillips GN, Jr. (2004) Structures and analysis of highly homologous psychrophilic, mesophilic, and thermophilic adenylate kinases. *J Biol Chem* **279**, 28202–8.
- Bae E and Phillips GN, Jr. (2005) Identifying and engineering ion pairs in adenylate kinases. Insights from molecular dynamics simulations of thermophilic and mesophilic homologues. *J Biol Chem* **280**, 30943–8.
- Bae E and Phillips GN, Jr. (2006) Roles of static and dynamic domains in stability and catalysis of adenylate kinase. *Proc Natl Acad Sci U S A* **103**, 2132–7.
- Bae E, Bannen RM, and Phillips GN, Jr. (2008) Bioinformatic method for protein thermal stabilization by structural entropy optimization. *Proc Natl Acad Sci U S A* **105**, 9594–7.
- Berman HM, Westbrook J, Feng Z, Gilliland G, Bhat TN, Weissig H, Shindyalov IN, and Bourne PE (2000) The Protein Data Bank. *Nucleic Acids Res* **28**, 235–42.
- Chan CH, Liang HK, Hsiao NW, Ko MT, Lyu PC, and Hwang JK (2004) Relationship between local structural entropy and protein thermostability. *Proteins* **57**, 684–91.
- Chen VB, Arendall WB, 3rd, Headd JJ, Keedy DA, Immormino RM, Kapral GJ, Murray LW, Richardson JS, and Richardson DC (2010) MolProbity: all-atom structure validation for macromolecular crystallography. *Acta Crystallogr D Biol Crystallogr* **66**, 12–21.
- Daniel RM and Danson MJ (2010) A new understanding of how temperature affects the catalytic activity of enzymes. *Trends Biochem Sci* **35**, 584–91.
- Eijssink VG, Bjork A, Gaseidnes S, Sirevag R, Synstad B, van den Burg B, and Vriend G (2004) Rational engineering of enzyme stability. *J Biotechnol* **113**, 105–20.
- Emsley P and Cowtan K (2004) Coot: model-building tools for molecular graphics. *Acta Crystallogr D Biol Crystallogr* **60**, 2126–32.
- Liszka MJ, Clark ME, Schneider E, and Clark DS (2012) Nature versus nurture: developing enzymes that function under extreme conditions. *Annu Rev Chem Biomol Eng* **3**, 77–102.
- McCoy AJ, Grosse-Kunstleve RW, Adams PD, Winn MD, Storoni LC, and Read RJ (2007) Phaser crystallographic software. *J Appl Crystallogr* **40**, 658–74.
- Moon S, Bannen RM, Rutkoski TJ, Phillips GN, Jr., and Bae E (2014a) Effectiveness and limitations of local structural entropy optimization in the thermal stabilization of mesophilic and thermophilic adenylate kinases. *Proteins* DOI: 10.1002/prot.24627.
- Moon S, Jung DK, Phillips GN, Jr., and Bae E (2014b) An integrated approach for thermal stabilization of a mesophilic adenylate kinase. *Proteins* **82**, 1947–59.
- Murshudov GN, Vagin AA, and Dodson EJ (1997) Refinement of macromolecular structures by the maximum-likelihood method. *Acta Crystallogr D Biol Crystallogr* **53**, 240–55.
- Otwinowski Z and Minor W (1997) Processing of X-ray diffraction data collected in oscillation mode. *Method Enzymol* **276**, 307–26.
- Vagin A and Teplyakov A (2010) Molecular replacement with MOLREP. *Acta Crystallogr D Biol Crystallogr* **66**, 22–5.